

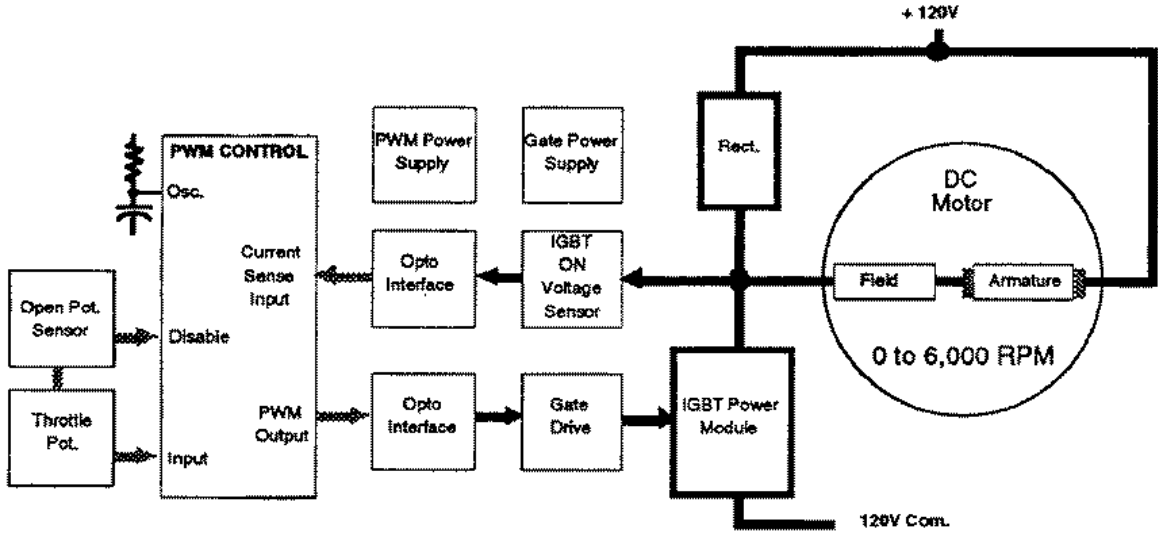
DC Motor Control For Electric Vehicles

Richard Valentine
Principal Staff Engineer
Automotive Segment Engineering
Motorola Semiconductor Products Sector
(revised March 15th, 1993)

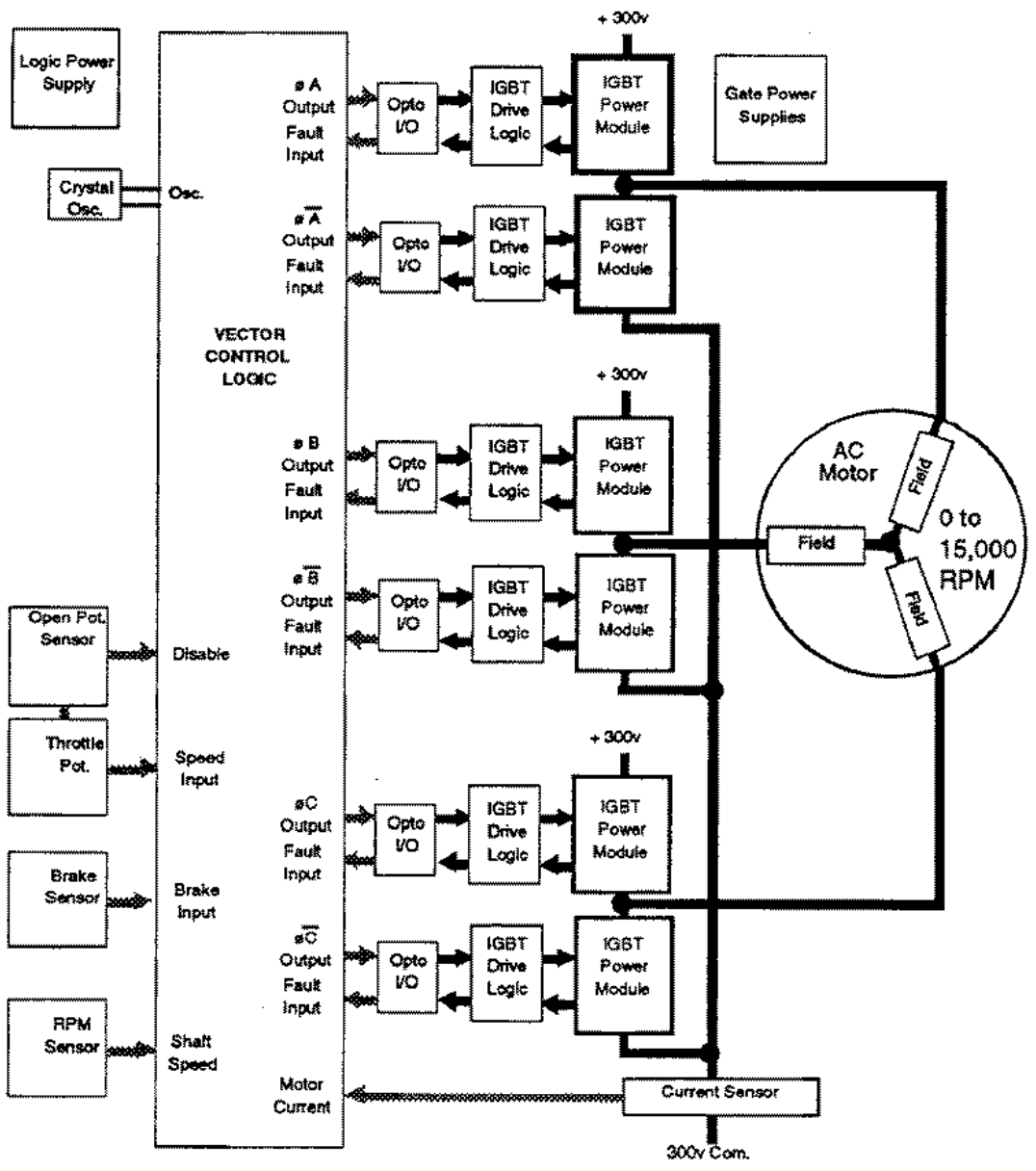
The design of an EV (electric vehicle) traction motor controller that switches 100,000 watt power levels with 1400 watt rated power transistor modules presents many challenges. Operating frequencies beyond a few kiloHertz are especially troublesome due to the motor's intrinsic inductance and the controller's high dv/dt values. The power transistor module's heat dissipation requirements necessitate the use of large air or liquid cooled heatsinks. Design criteria, and a working circuit for a DC motor controller are reviewed along with suggestions for future component improvements. (This experimental motor control design, while not production rated, has been used successfully in a high performance electric race vehicle ¹.)

Electric Vehicle Motor Control. The motor control regulates the motor's speed and limits the motor's maximum current level. The motor speed range can vary from zero to wide open throttle (WOT), which requires the controller's power transistors to sustain high peak currents and provide good efficiency at nominal cruise speeds. The controller also has to be self-protecting against electrical disturbances such as an intermittent battery cable or a faulty throttle position sensor. There is also a significant heat transfer requirement from the controller's power transistor modules that requires a large heatsink with auxiliary fan cooling or a liquid cooled heatsink that may also be tied in with the electric motor cooling system. Other aspects of the motor controller design include detection of excessive heatsink or motor temperatures, and diagnostic readouts.

The traction motor category determines the type and cost range of the controller. Pulse width modulation (PWM) type controllers are often used with brush type DC motors which have been successfully applied for many years in fork-lifts and electric vehicle conversions. AC powered motors for EVs require a motor controller that not only regulates speed, but must also generate AC drive voltages from the DC battery supply. Generally, the AC motor electronics will be four to six times more complex than the DC motor controller. AC motors however can operate at higher battery supply voltage levels, which reduces the power transistor's current levels. The block diagram shown in **Figure 1** compares a DC brush motor and a three phase AC motor drive.



DC Brush Motor



AC Induction Motor

Figure 1. Motor Type Comparison

The DC motor system was chosen for this controller design because of its intrinsic higher reliability factor, as compared to the "Totem-Pole" or half H bridge design used for AC drive systems. A glitch in the DC motor drive signal may cause a slight roughness in the motor speed, while the same glitch could permanently destroy the AC drive system by turning on both top and bottom devices at the same time. AC motor controllers demand more sophisticated power devices that can protect themselves against erroneous control signals or harsh motor faults. Once these self-protected power devices are commercially available at a total system price of somewhat less than the motor, then AC motors will probably be preferred over the present day DC motors as the motor of choice for EVs. The controller circuit design criteria to be described can apply to either AC or DC controllers.

DC Motor Control. The series wound DC motor and control trades simplicity and low cost for wide speed range performance as compared to AC variable speed motor systems. The DC series wound motor offers formidable torque in the 0 to 2,000 rpm range, while special designed AC motors can produce high torque all the way to 15,000 RPM². The DC series wound motor's speed is controlled by altering the average voltage to the motor by pulse width modulation (PWM) at a fixed frequency. This speed control method (also called chopping) relies upon the motor's inductance to integrate or smooth out the PWM pulses. The main drawback to this method is that the entire motor current must be modulated, and in the case of a 100kW rated motor, current levels in the 1,000 amp range are required. This high current demand leads to the use of three parallel connected 400A/600V power transistor modules. By choosing IGBT (Insulated Gate Bipolar Transistors) type modules, the gate drive power requirements can be kept under 5 watts. Other types of power devices were considered, such as bipolar darlingtontons and MOSFETs, but as shown in Table 1, the IGBT technology offers the best overall high current performance based upon switching speed, gate drive power and ON voltages. The high voltage darlington requires substantial base drive current, 2 to 25A, to maintain a low VCEon from 100A to 600A, and has poor switching times. High voltage MOSFETs exhibit high VCEon, requiring ten or more in parallel, while four paralleled lower voltage rated MOSFET devices perform well as shown in Figure 2 when operating from a 120 volt battery supply.

Device Type	Qty ea.	ON Voltages*			Switching*			Driver Requirement*
		100A	400A	600A	Ton	Tstr	Tfall	
600V Darlington	1	0.95V	1.5V	2.0V	3µs	8µs	0.6µs	2.7V @ 2/8/25A
600V IGBT	1	1.85V	2.5V	3.0V	0.3µs	1µs	0.2µs	15V @ .04A
500V MOSFET	10	1.0V	4.0V	6.0V	0.3µs	0.4µs	0.2µs	20V @ .04A
150V MOSFET	4	0.52V	2.1V	3.15V	0.2µs	0.2µs	0.1µs	20V @ .04A

*estimated

Table 1. Comparison of Power Modules.³

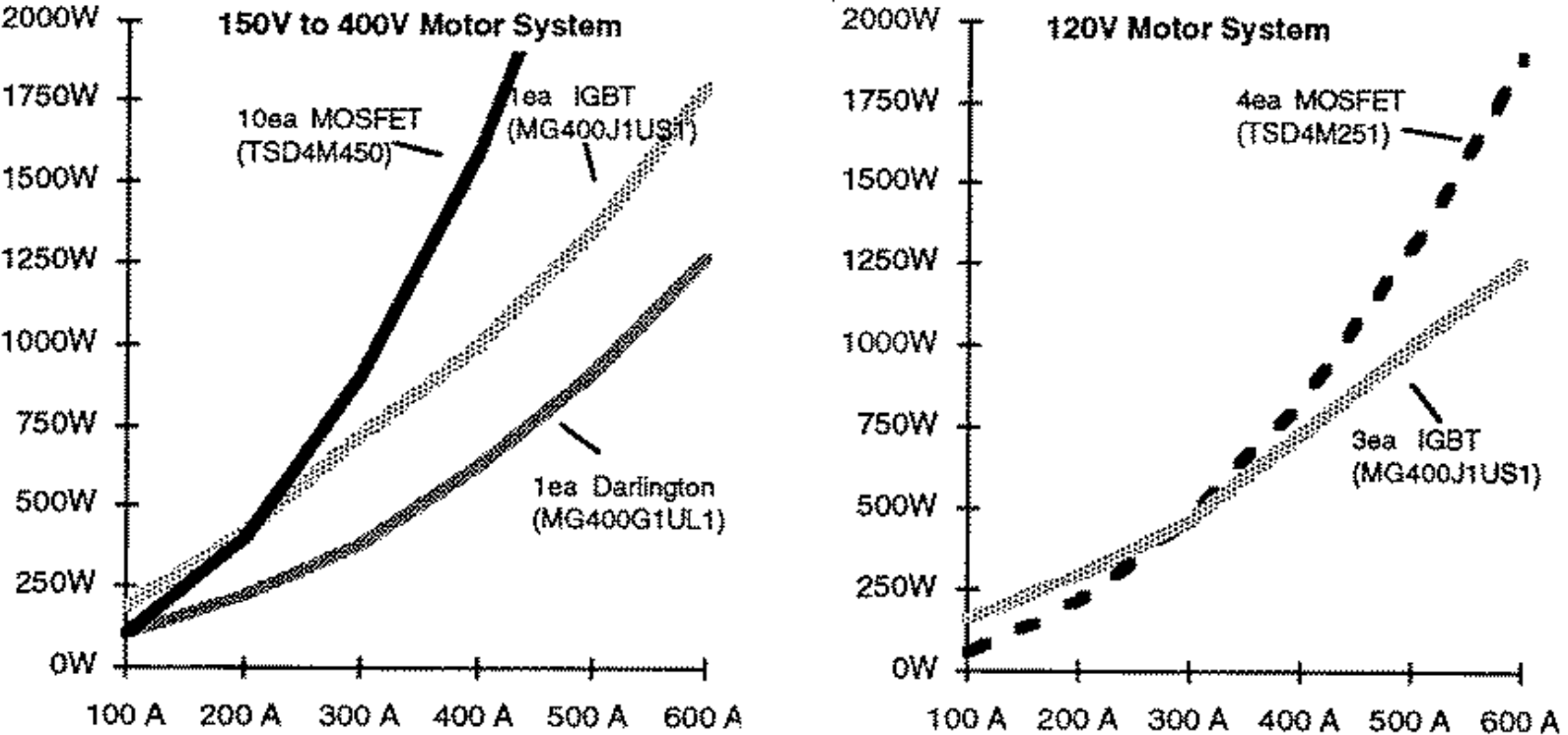


Figure 2. Power Module DC Dissipation

PWM Speed Control Considerations. Since the EV motor is a dynamic machine with the armature and powertrain acting as a flywheel, the voltage interruption or chopping rate could be 1,000 Hertz or slower, before the vehicle's speed actually pulsates. What is a problem at 1,000 Hz or other audible rates is noise generated from within the motor. This audible motor sound may not be tolerable for drivers or passengers. At higher frequencies, 16kHz or greater, the audible noise is minimized. Another noise issue is the significant electronic radio frequency interference (RFI) that radiates into the electrical system including the vehicle's radio equipment. This RFI is generated by the fast switching edges of the PWM signal. Slowing down the switching edges minimizes the radio frequency interference (RFI), but the switching speed parameters also play a crucial role in the overall controller system. High transitional speeds are desirable to minimize switching losses and improve reliability, but very fast switching speeds become impractical beyond a certain point due to the inherent inductance in the wire and component leads. A compromise has to be made between the edge speeds and power device heat loss. The drawing in Figure 3 illustrates the switching speed and power transistor dissipation relationship at a fixed operating frequency.

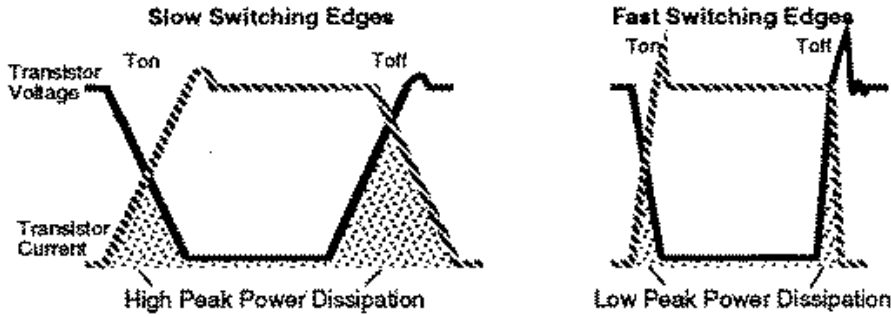


Figure 3. Voltage-Current Relationship vs Switching Speed.

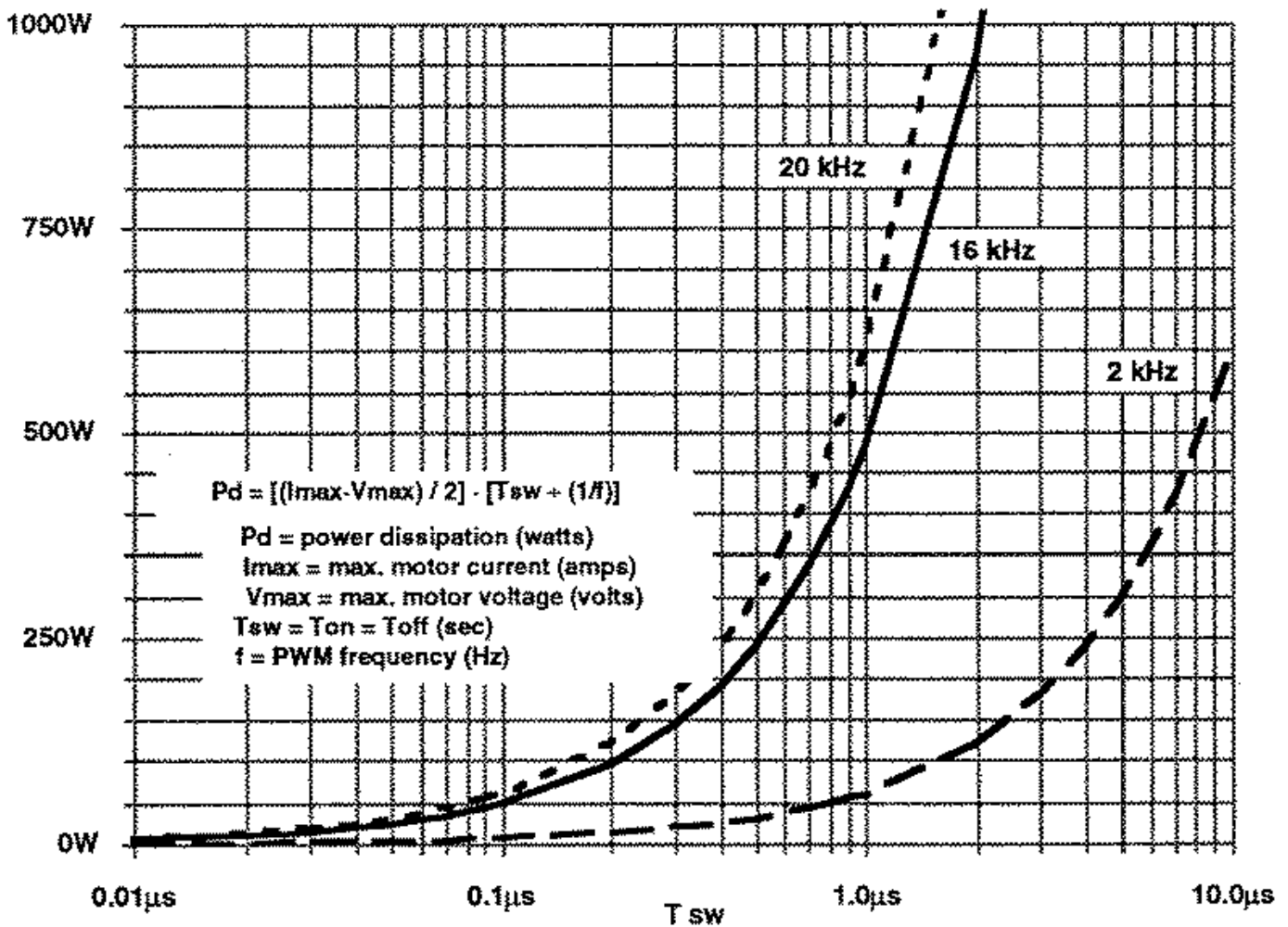


Figure 4. Switching Speed Effects Upon Power IGBT Module Dissipation

Figure 4 graphs the switching edge speed effect upon the power transistor's power dissipation when switching a 400 amp motor load from a 150 volt power supply. Three different operating frequencies are plotted, one at 20kHz, 16kHz and the last at 2kHz. Note how the 2kHz switching times are less critical than the higher 16 and 20kHz

frequencies. In order to minimize audible noise, the 16kHz frequency was chosen for this experimental controller, but, unfortunately, the 100 to 300 nanoseconds switching speeds required to maintain reasonable switching loss cause the intrinsic inductance in the hookup wiring, components, and motor to become critical. These faster edge speeds will generate significant voltage spikes across the hookup wiring, and may lead to reliability problems unless precautions are made to minimize stray inductance in this wiring.

Effects of Inductance. If the motor controller's lead lengths exceed 1 inch (25mm) then their inductance values must be taken into account. An inductance value of $0.1\mu\text{Hy}$ can be obtained in about 6 inches (152mm) of wire length with a #1/0 wire size as shown in Figure 5. This $0.1\mu\text{Hy}$ value may not sound like much, but a plot, Figure 6, of power line inductance versus switching transition times, shows that just $0.1\mu\text{Hy}$ of lead inductance can generate an 100 volt voltage spike (at 400 amps motor current) when switching edges are about $0.4\mu\text{s}$. Therefore if fast switching edges are to be used, as with a 16 kHz operating frequency, then a capacitor filter network is mandatory near the motor's power lead, and controller. This filter network actually has to smooth out both the 16 kHz, and the much higher frequencies associated with the 200 to 1,000 nano-second switching edges.

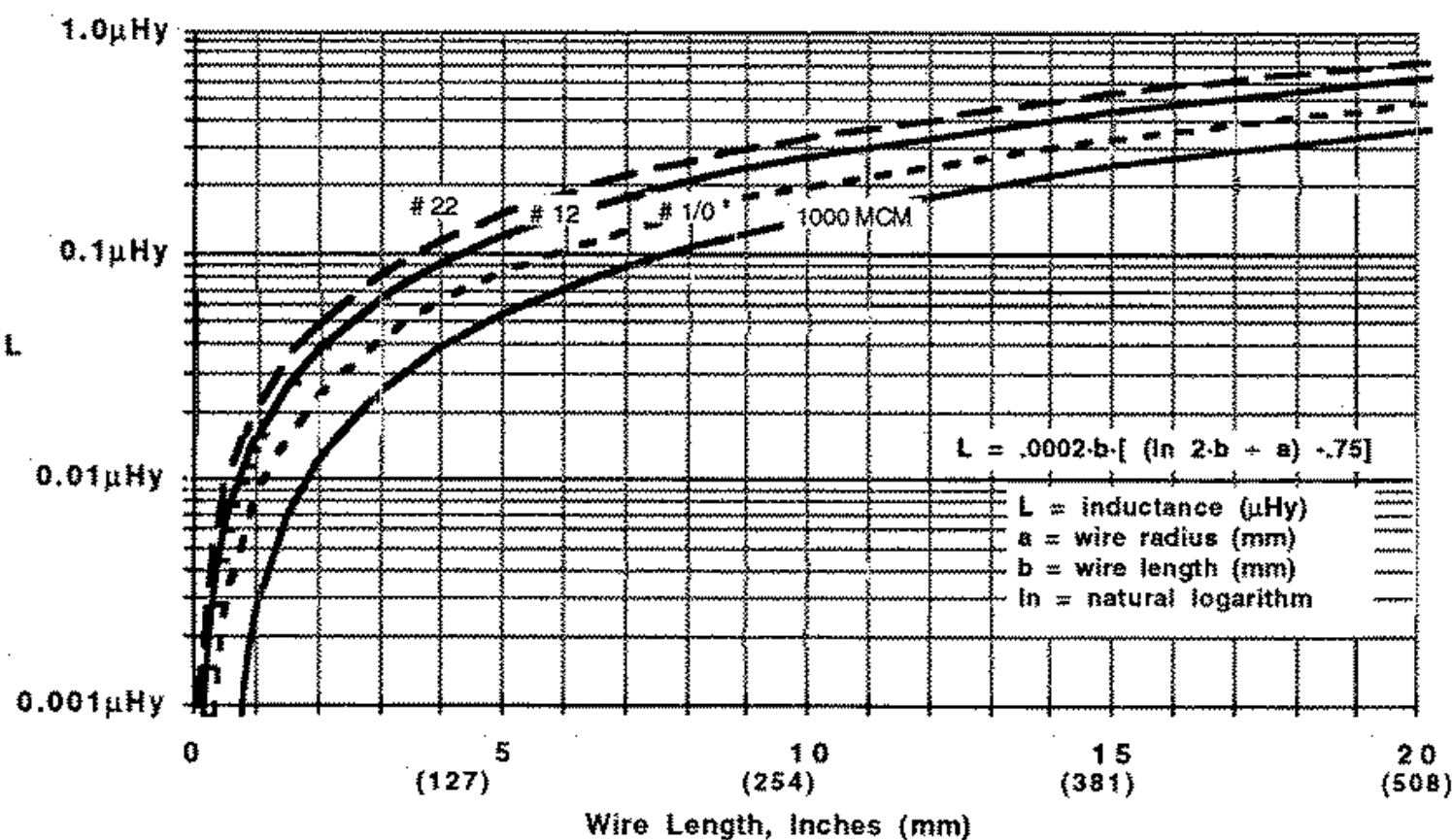


Figure 5. Straight Wire Inductance⁴

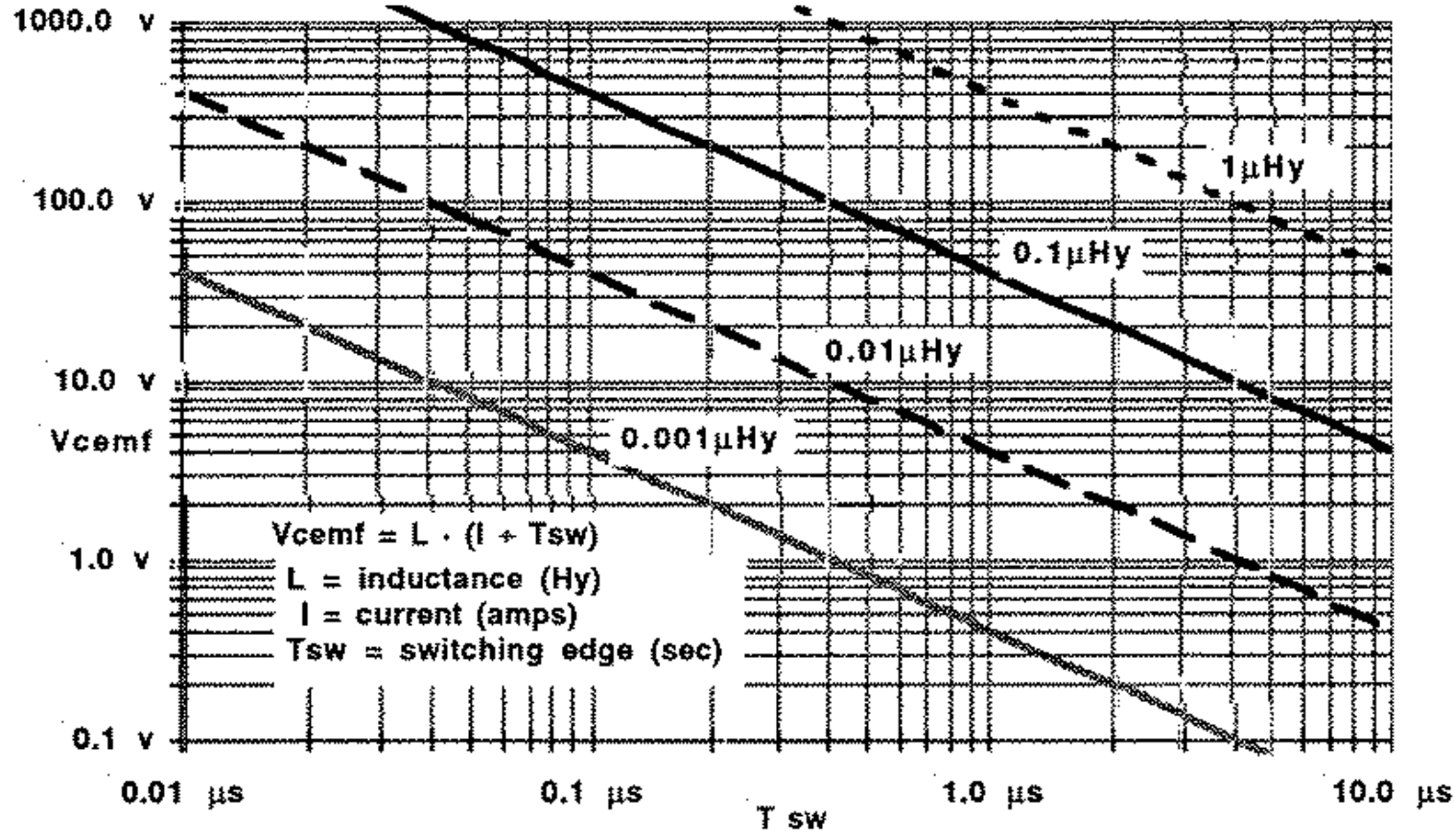


Figure 6. Switching Speed vs. V_{cemf}

The high frequency capacitor network's performance is largely determined by the selection of capacitors that are capable and specified to operate at high DV/Dt rates⁵. The interconnections between both the large electrolytic type capacitors, the smaller metallized film units, IGBT modules and free wheeling rectifiers (FWT) should be short, but wide copper plates, to minimize inductance. Figure 7 shows a good vs. poor layout for the capacitors and other associated devices in the controller. Note how the good layout is also the most compact.

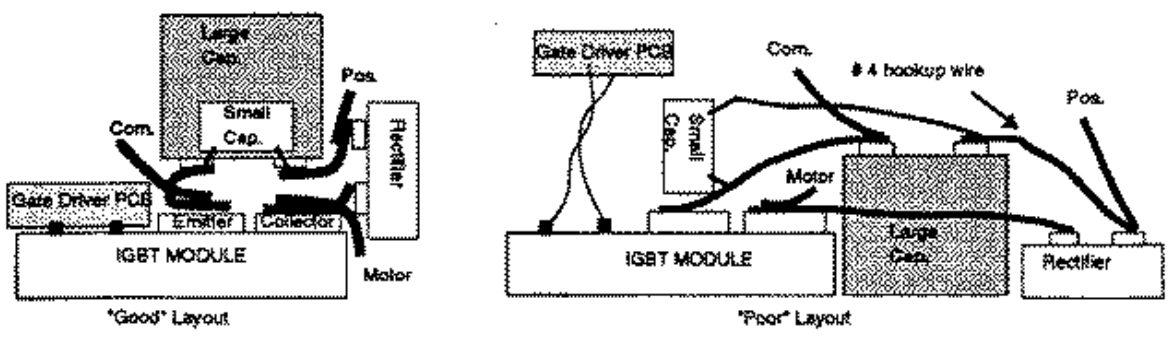


Figure 7. Construction Layout

Motor Winding Inductance. The kickback voltage from the motor's inductance also has to be contained, as the motor's inductance value will be dominant over the hookup wiring and bus bars. This high energy laden voltage spike must be dealt with or else the power transistor will enter an avalanche or second breakdown mode, which is something to be avoided. The energy content of the motor's inductive kickback voltage is mostly determined by the motor's current, the motor's internal and external wire inductance value, and the rate at which the current is switched off. A high current rated freewheeling rectifier network is connected across the controller's battery and motor terminals to clamp the motor's inductive kickback voltage spike. The reverse recovery time of these freewheeling rectifiers do affect the IGBT's switching performance.

When operating at a frequency of 16kHz or a 63μs repetition rate, the motor's inductance value is large enough to keep the freewheeling rectifier in a forward conduction mode until the next 63μs cycle occurs. For example, if the PWM is set to a 25% duty cycle, then the IGBT is on for the first 16μs, and the freewheeling rectifier is in conduction for the remaining 47μs. This means that when the next cycle occurs, the IGBT is switching on while the freewheeling rectifier is still in conduction. The result is that the IGBT and freewheeling rectifier conduct a high level "shoot through" current spike. The magnitude and duration of this current spike is directly related to the rectifier's reverse recovery time rating, lead inductances, and the battery supply source impedance at the rectifier and IGBT location.

Motor Current Control. Once the motor's inductive voltage spikes are safely contained, the stalled and shorted motor conditions need to be dealt with. Using a typical DC EV motor⁶ as the load, the maximum stalled or locked rotor current can be calculated as shown below.

$$\begin{aligned}
 I_{\max} &= E_{\max} \div R_{\text{mtr}} & E_{\max} &= \text{maximum power supply voltage} \\
 &= 120 \div 0.05 & R_{\text{mtr}} &= \text{minimum motor (.04}\Omega\text{) and hookup wire (.01}\Omega\text{) resistance} \\
 &= 2400\text{A}
 \end{aligned}$$

A 2400 ampere current level is well beyond the motor's safe limit of operation, and will result in brush assembly destruction and/or severe winding overheating. Therefore a maximum value of motor current has to be established that still allows reasonable torque and safe motor operation. Another factor to consider, is the diminishing driving range as the maximum motor current level is increased. The type of driving cycle will greatly affect this tradeoff; high rates of maximum WOT during stop-and-go traffic vs. constant speed open country type driving. Since it is not practical to select devices that can sustain the maximum energy levels that occur during a catastrophic motor failure (a dead short for

example), a current limiting design becomes a necessity even if the motor and controller could sustain 2400 ampere levels. This same current limiting design can also be used to limit the motor's peak current level during WOT, and a locked rotor condition. For this experimental design, the maximum motor current can be adjusted from 300 to over 900 amperes, thereby allowing the driver to trade performance for distance. 300 ampere current levels give fair EV performance; acceleration times from 0 to 40 mph (0 to 64 km/h) are a sluggish 15 plus seconds while 900 ampere levels allow the EV to approach the performance levels of a small 4 cylinder gasoline engine⁷.

Power Dissipation. A prime consideration for reliable power transistor module operation is heat dissipation. The worst case scenario would include maximum values for the ambient temperature, heatsink thermal resistance, contact thermal resistance from heatsink to transistor module, and the transistor module's case to junction thermal resistance. The equation below calculates the power transistor's maximum allowable heat dissipation during WOT. This equation is for a wide open throttle condition. A maximum junction temperature of 150°C for the power transistors was chosen. It should be noted that the reliability will increase by about one order of magnitude for each 10°C drop in the power transistor's junction temperature. The heatsink's .03°C/W thermal resistance value represents either a large forced air cooled heatsink or a smaller sized liquid cooled heatsink unit.

$$\begin{aligned}
 P_{Dmax} &= (T_{Jmax} - T_{Amax}) \div (R_{\theta JC} + R_{\theta CS} + R_{\theta SA}) \\
 &= (150 - 40) \div (.08 + .025 + .03) \\
 &= 815 \text{ watts per module}
 \end{aligned}$$

T_{Jmax} = maximum allowable junction temperature

T_{Amax} = maximum ambient temperature

$R_{\theta JC}$ = junction to case thermal resistance

$R_{\theta CS}$ = case to heatsink interface thermal resistance

$R_{\theta SA}$ = heatsink to ambient thermal resistance

After the maximum module power dissipation allowance is known, which is about 800 watts or 2400 watts for three modules, then each module's forward voltage drop, V_{CEon} , and ON resistance can be calculated as shown below. Three 400 ampere IGBT modules connected in parallel easily meet the 900 ampere current requirement provided they are selected for good matching, and correctly mounted onto a very good thermally efficient heatsink.

$$\begin{aligned}
 V_{CEmax} &= P_{Dmax} \div I_{max} \\
 &= 800 \div 300 \\
 &= 2.67 \text{ volts at } 150^{\circ}\text{C } T_j
 \end{aligned}$$

$$\begin{aligned}
 R_{CE \max} &= P_{D\max} + I_{\max}^2 \\
 &= 800 + 90,000 \\
 &= .009 \text{ ohms at } 150^\circ\text{C } T_j
 \end{aligned}$$

A 2.67 volt forward ON voltage specification at a 300 ampere nominal current level can be met by several commercially available 400A IGBT modules⁶.

IGBT Drive Considerations. Driving one IGBT power module is simple as compared to driving several in parallel. The difficulty lies in the gate drive connections as they allow a second high current path to occur when the emitter-kelvin connections are all tied in parallel. Through experimentation with the emitter-kelvin contacts and the gate driver circuits, it was found that a stable turn-on waveform would be obtained when a large copper plate was tied across all three emitter-kelvin contacts and the high current emitter contacts. Selecting an IGBT module that has minimal internal emitter lead inductance will help to avoid oscillations that occur during the turn-on time of the IGBT. The root cause of the oscillation can be traced to the reverse recovery time of the freewheeling rectifier across the motor that is used to clamp the turn-off voltage spike generated by the motor's internal winding inductance. Because of the motor's winding inductance time constant with respect to the 16kHz switching frequency, the freewheeling rectifier is in conduction during the off time of the power IGBT modules. When the power IGBT modules are switching on, the freewheeling rectifier has to clear, which in effect, shorts out the main battery rail to common for a brief moment, usually less than 100ns. This very high current level causes the emitter leads to create a voltage spike that opposes the gate drive signal, and begins to turn off the device. This event happens at a 10 to 30 ns repetition rate and lasts for about 50 to 100 ns or until the rectifier has finally cleared.

The selection of a freewheeling rectifier with a recovery time specification similar to the IGBT turn-on time appears to minimize the unwanted turn-on oscillation problem. The use of 20 to 30 nanosecond reverse recovery rectifiers was found to be especially troublesome with IGBTs that have high internal emitter lead inductance. This problem intensifies when the IGBTs are connected in parallel.

PWM Circuit Design. The circuit shown per Figure 8 was developed to control a 9" diameter DC motor. The PWM control is based upon a single bipolar linear IC that was originally designed for controlling 3 ϕ brushless motors. This part was primarily chosen because of its ability to operate from 0 to 100% PWM while maintaining an over current function even at 100% duty cycle, and is characterized for motor control. The circuit operation can be broken down into several functions: the PWM control, speed control fault

detector, PWM output to gate driver opto interface, gate drivers, IGBT VCEon sense opto interface, power IGBT control, heatsink temperature sensor, gate drive power supply, and 12V regulator.

PWM control. The throttle control pot is connected to supply an analog voltage that is proportional to its position. The pot's output voltage to the controller IC input varies from about .85v at zero speed to 4.1v at WOT. The PWM signal varies from 0% at .85V to 100% at 4.1V input. A low pass filter on the pot control line reduces any spurious noise on the speed signal, and allows the addition of a simple resistor-capacitor (RC) acceleration rate limiter. The maximum throttle acceleration rate is set to about .3 seconds. To insure fast deceleration response from the controller, a diode was added across the resistor part of the acceleration rate RC network which will discharge the capacitor quickly when the throttle goes to zero position. The PWM oscillator 16 kHz frequency is set by the RC values tied to the controller OSC pin. The selection of a temperature stable capacitor maintains an accurate frequency over extreme temperatures. Most ceramic type decoupling capacitors, while inexpensive, are not adequate, and a mica or similar capacitor with minimal temperature drift should be used.

Speed control fault detector. One potential safety issue with any motor control system is a runaway speed condition due to a broken/loose wire or an open throttle control device. A throttle pot current sensor was added to detect an open circuit in the throttle pot or its low side interconnection. The throttle fault sensor uses a comparator and monitors the voltage drop across a resistor on the low side of the throttle control. If this voltage drop goes to zero, or below the comparator's reference of .05v, then the comparator output toggles low, and disables the PWM output. A LED indicator is also turned on to visually indicate the throttle fault condition. An open line on the throttle control's center lead is controlled by a pull-down resistor on the PWM input line near the control IC input pin.

PWM output to gate driver opto interface. The PWM control IC output signal is connected to the input side of an opto-coupler device. A 5.1v Zener shunt regulator was added to maintain a constant current to the opto-coupler. This insures the opto-coupler's output signal remains stable during varying power supply conditions, such as when the 12 volt battery line slowly goes from 13.6v at full charge to 11v when its charge is nearly exhausted. There is a 10 volt under voltage lockout (UVLO) circuit built into the control IC that disables its output if the 12 volt battery goes below 10v. The opto-coupler shown is a Schmitt logic type, which tends to minimize noisy signals at the expense of a reduced response time. A delay time and minimal pulse width of about 1.5 μ s was observed. This means that the minimal PWM signal can only be 1.5 μ s which is a good number to work with, as it matches the switching speed response of the IGBT output stage. A narrow 0.5 μ s

pulse, would not allow the IGBT to switch fully ON and will stress the IGBT in a forward bias safe operating mode (FBSOA). Even though these IGBTs are rated at 400A, they have limited power capability in the linear mode of operation, less than 1A at 100VDC.

Gate drivers. The opto-coupler inverted output signal is connected to each IGBT gate driver printed circuit board (PCB). The gate driver PCB is mounted directly on top of each power IGBT module. The gate driver uses a MOSFET driver IC to drive a complementary MOSFET amplifier stage. This stage is capable of switching the 5 to 7 amp peak gate current levels required to charge and discharge the large 40,000 to 80,000 pf IGBT gate capacitance in less than 500 nanoseconds. The series gate resistors values largely determine the switching speed of the gate voltage. It is possible to slow down the turn on time by increasing the upper P MOSFET resistor's value, and to increase the turn off time by lowering the N MOSFET resistor value. The gate resistors should be flame-proof types to minimize PCB damage in the event of an IGBT collector to gate short.

IGBT V_{CEon} sense opto interface. The IGBT module's current level is sensed by measuring the IGBT transistor's forward ON voltage. This method does have some inherent drawbacks. The collector to emitter voltage measurement circuit has to be synchronized with the gate drive voltage, and the V_{CEon} will vary over temperature. A temperature compensator added into the current limit detection circuit minimizes the temperature drift problem, and a simple transistor stage synchronizes the current sensor stage. A closer look at the current sensor design shows that the IGBT's ON voltage value plus a diode drop appears at the comparator's negative input. Normally this voltage will vary from 1.5 volts during minimal motor load to over 3.5 volts during WOT or a stalled motor condition. The comparator's reference positive input determines the trip point. A current limit range of 300 to 900 amperes is obtained by varying this reference input voltage from about 2.6 to 3.6 volts. A NPN bipolar transistor mounted near the IGBT modules is used for temperature compensation. This is required because the IGBT ON voltage (with the current held constant) will vary with a slightly negative coefficient. Unfortunately the coefficient factor varies with different IGBT brands as shown in **Figure 9**. If no temperature compensation is used then the maximum current level will increase as the IGBT modules heat up. This causes a regenerative action; more current will then flow, additionally heating up the modules, leading to more current flow which eventually causes a burned out motor or failed IGBT module. It is possible to increase the temperature compensation factor to purposely reduce the motor current as the modules heat up thereby decreasing the chance of a heat induced failure.

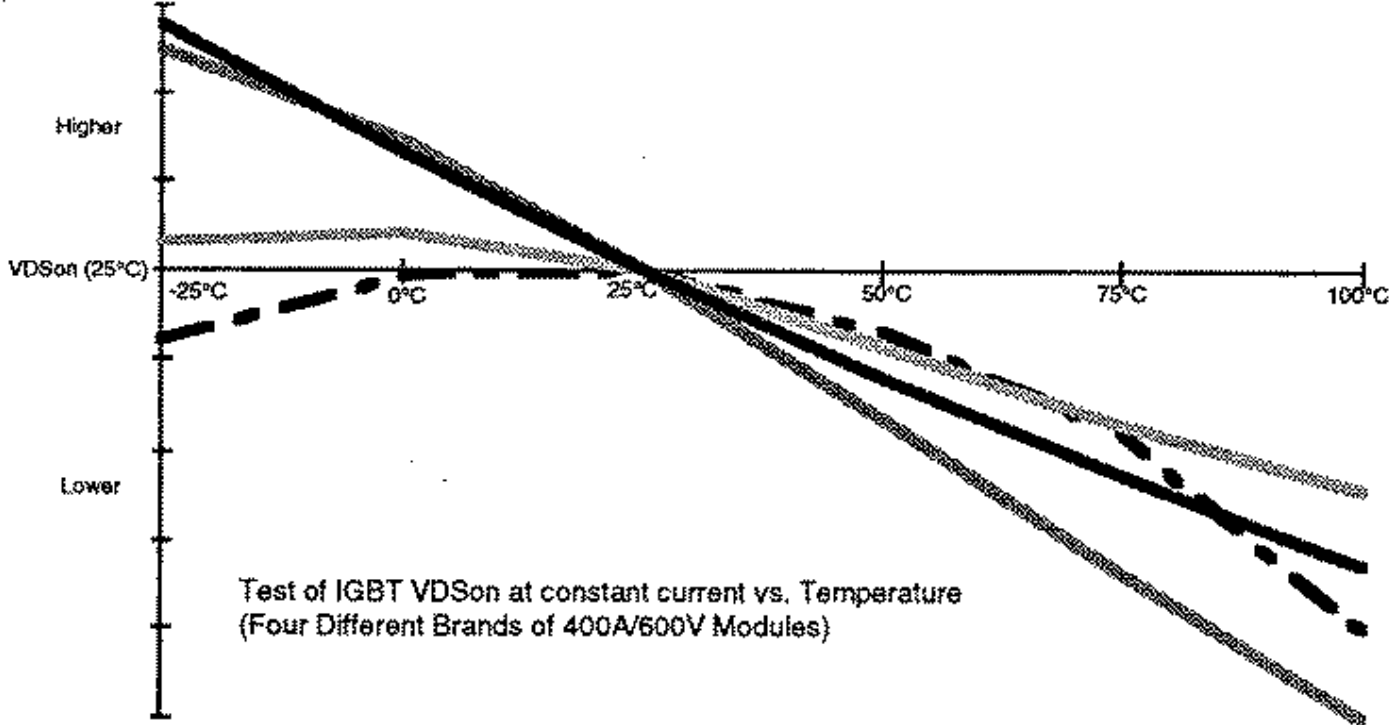


Figure 9. IGBT VCEon Variation over Temperature

Power IGBT control. Three 400A/600V fast IGBT power modules are connected in parallel with large copper or aluminum buss bars. Several 100ns “soft” fast recovery rectifiers are connected in parallel in close proximity to the IGBT’s collector terminals and the battery/motor+ bus bar. The high frequency 2 μ f/400V metallized film capacitors, and the large 3300 μ f/250V low ESR (equivalent series resistance) electrolytic capacitor are also in close proximity to the battery/motor+ and battery common bus bars. It is a good idea to match the IGBT devices for similar VCEon values over their 100 to 300A range. This will help equalize current sharing amongst all three units. One important item is the proper mounting of the IGBT modules to the heatsink. The thermal interface between the module’s case and the heatsink must be kept as low as possible or else excessive junction temperatures will be incurred under WOT. The modules should be mounted with either non-drying silicone thermal grease or a metallized silicone pad⁹. The heatsink mounting area should be held under .001" (.0254mm) flatness, plus the module heatsink fastener’s torque values should be verified with a torque gauge. As a final precaution against voltage spikes, voltage clamping networks such as metal oxide varistors (MOVs) across the IGBTs and freewheeling rectifiers insure that these devices will not be destroyed by other excessive voltage spikes that may occur due to intermittent wire connections.

Heatsink temperature sensor. Protection against excessive heatsink temperatures is accomplished with a NPN bipolar transistor connected as a base-emitter diode mounted to

the heatsink. Two comparators monitor its base-emitter voltage. One comparator is set to trip at a voltage that is equal to $+20^{\circ}\text{C}$ and controls the heatsink's cooling fans. A feedback resistor allows a 5°C hysteresis factor, which means once the fans are on, then the heatsink has to cool off to $+15^{\circ}\text{C}$ before they turn off again. The second comparator is set to trip if the heatsink temperature rises above 75°C . If this happens, then the PWM control input voltage is reduced to reduce the PWM, which reduces the heatsink's excessive temperature. A resistor from the comparator's output is used to pull down the PWM voltage input level thereby limiting the PWM. The value shown limits the PWM to 50% at WOT.

Gate drive power supply and 12V regulator. The vehicle's 12 volt battery supply was chosen to power the controller's analog functions mainly for simplicity. As required by any electronic equipment running off a 12V battery system, protection against reverse battery hookups, excessive charging voltages, and intermittent battery connections must be accounted for. A rectifier protects against reverse battery hookups, a series resistor establishes a maximum current level, and a $3,000\mu\text{f}$ capacitor forms a large RC filter network. A 20V zener was added to protect against excessive voltage on the 12V filtered output. There is another reason to add the large $3,000\mu\text{f}$ capacitor, and that is to insure the controller's operation remains stable when the 12V line is switched ON-OFF-ON-etc. in a rapid fashion. A small internal 12VDC to 15VDC convertor is used for the gate driver's +15 volt supply. It is necessary to provide an isolated power source to the IGBT power control because of its electrical noise levels, and to electrically isolate the throttle control plus diagnostic functions from the battery supply. The +15V DC output matches most IGBT specification sheets for a nominal gate bias voltage. Lower V_{CEon} values can be obtained with a 20V gate bias level but with a reduction in short circuit capability of the IGBT¹⁰. In retrospect a better method would have been to use two internal high voltage 50V-to-200V DC to +15V DC converters. One for the analog functions, and the other for the IGBT drivers. This would insure the motor controller would operate as long as the main battery supply was operational. One aspect of powering the motor controller from the high voltage battery supply is to design the logic control circuits such that they always operate in a stable manner under wildly varying battery supply voltages.

Summary EV motor speed control can be accomplished using IGBT power modules. The present modules, however, are not optimized for EV environments, nor priced for the EV market. Future IGBT technology improvements will improve the price-performance aspect, while automotive specific designs will address the EV reliability issues.

A single chip microcontroller (MCU) could greatly enhance the operation of this design by allowing more functionality. For example, a stalled motor condition could be detected and a preset shutdown mode invoked to protect the motor against burnout. Other types of predetermined modes and functions could easily be accommodated with a small 8 bit type MCU. The MCU could monitor the motor battery voltage and current levels for use in calculating the average energy consumption rates and predict the remaining range of the vehicle. The main difficulty to using an MCU is its sensitivity to the RFI present in the motor controller. Careful printed circuit board layout (PCB), and RFI filters on the MCU's I/O lines are necessary plus metal shielding around the MCU PCB area. The metal shielding will also help to minimize the effects of mutual coupling from the very high magnetic fields created when the controller is operating at WOT.

Probably the single most difficult circuit function to design for the EV motor controller is a fast responding and accurate current sensor. An integrated current sensor in the module that would indicate the exact IGBT collector current level with less than 5 μ s delay to the control logic would simplify the motor controller design.

Acknowledgements. The author thanks the other members of the "GENESIS" team Jeff Baum, Ken Berrindger, Tom Huettl, Marko Koski, Dan Mason and Mark Torfeh for their contributions to this EV controller design.

References.

- 1 DEMI /APS Electric Saturn , 1992 Solar & Electric 500 Race, PIR, Phoenix Ariz.
- 2 M. Fukino, N. Irie and H. Ito: Development. of an Electric Concept Vehicle with a Super Quick Charging System, SAE 920442, Feb. '92
- 3 Toshiba POWER MOS FET & GTR MODULE Data Book, SGS-Thompson MOSFET Data Sheets
- 4 1988 ARRL Handbook, Chapter 2-18
- 5 Philips 3300 μ F-250V FH332T250DPA3 and 2 μ F-400V 378MKP capacitors
- 6 Advanced DC Motor Model FB-4001
- 7 EV is 1982 4 door Mercury Lynx powered by 100V 80A/hr lead-acid battery pak and Prestolite MTC4001 motor
- 8 TOSHIBA part # MG400J1US1, POWERX part # CM400HA-12E, FUJI part # 1MB1400L-060
- 9 BERQUIST Q-PAD II, thermal conductive material
- 10 FUJI IGBT MODULE APPLICATION MANUAL, REH 214a., p.8-9

For more reading on electric vehicle systems and components the following list of publications provide a wealth of information.

SAE International, SP-862, ELECTRIC VEHICLE DESIGN and DEVELOPMENT, 1991, 116 pps

SAE International, SP-880, ELECTRIC VEHICLE R&D, 1991, 67pps

Bradford Bates, ELECTRIC VEHICLES: A Decade of Transition, SAE International PT-40, 1992, 357 pps

SAE International, SP-915, ELECTRIC and HYBRID VEHICLE TECHNOLOGY, 1992, 91 pps

Gerry Kobe, "POINT of IMPACT", AUTOMOTIVE INDUSTRIES, July 1992, P40-43

M. Earle, F. Standish, D. Sloan, J. Tetherow, F. Wyczalek, "PROPULSION TECHNOLOGY: an Overview", AUTOMOTIVE ENGINEERING JULY 1992. VOLUME 100, Number 7, P29-33

Motorola Dual 225 Rectifiers)

IGBT POWER MODULE LAYOUT
 Back View cont'd
 Page 2 of 10

PRELIMINARY, Prototype Lab Test

PCB 7.9 X 4.4"

Capacitor
 Philips
 183-1511-080
 3120 FH332T250DPA3
 3300uf -10% +50%
 250VDC 300 Surge
 85°C Max Ambient

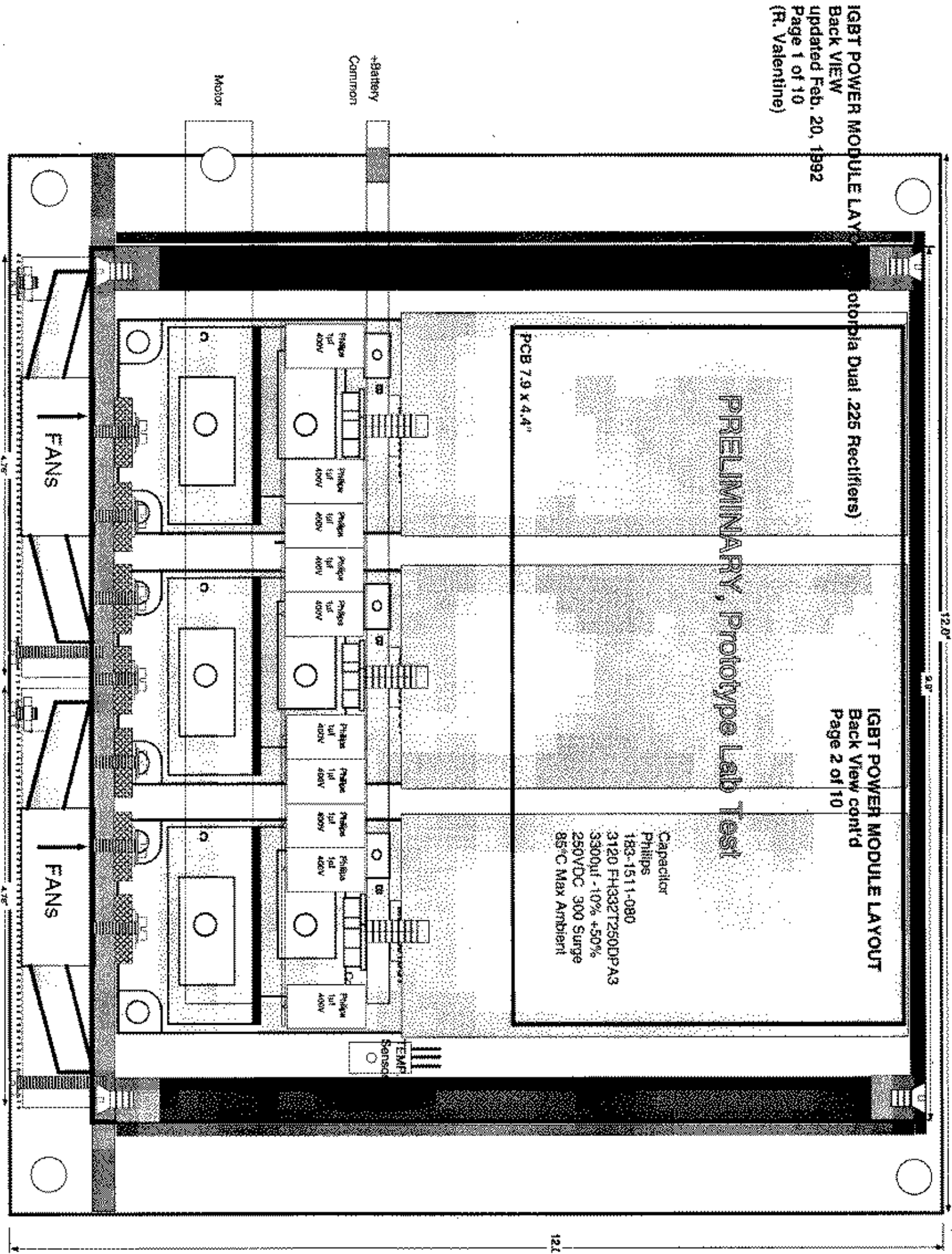
+Battery
 Cannon

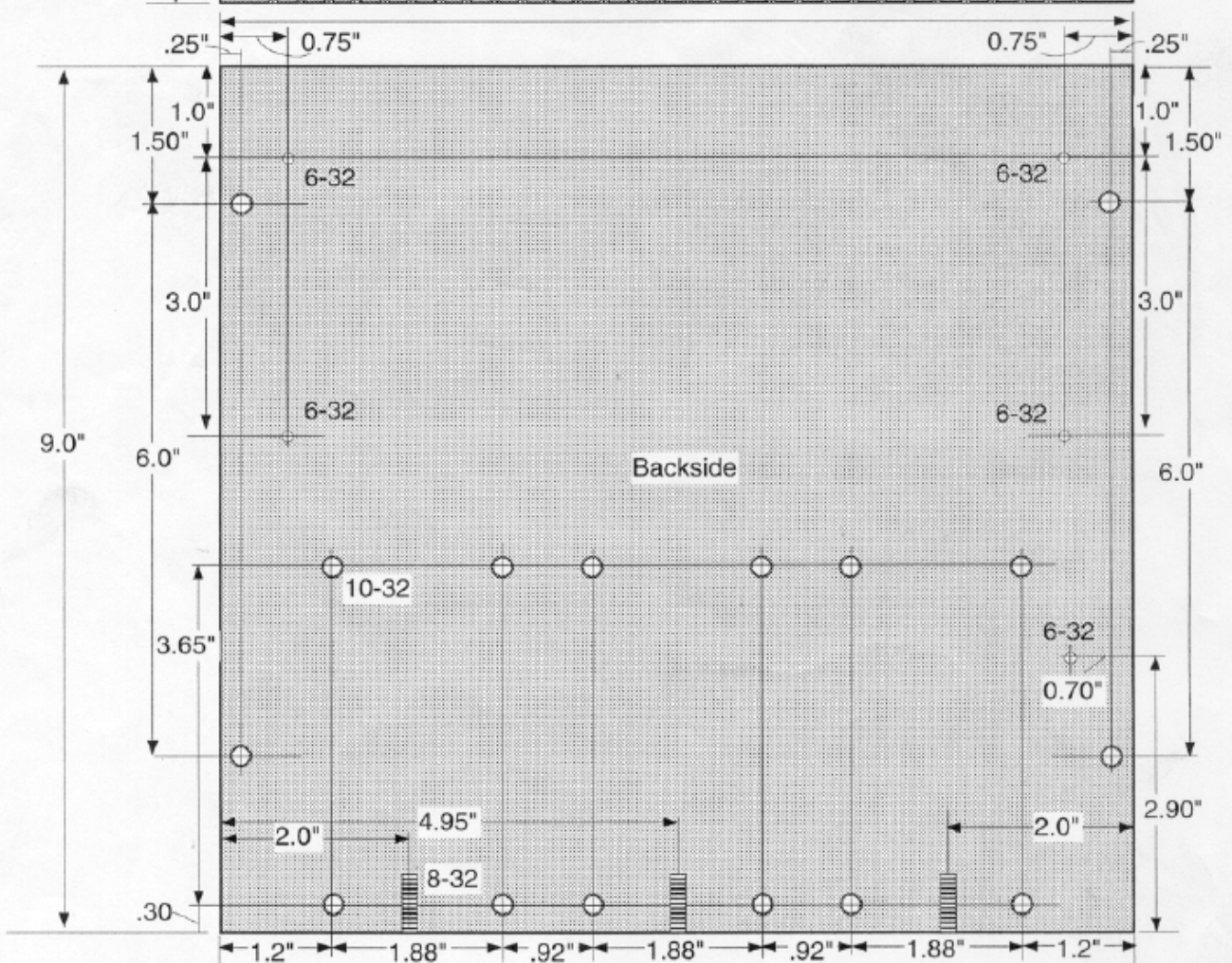
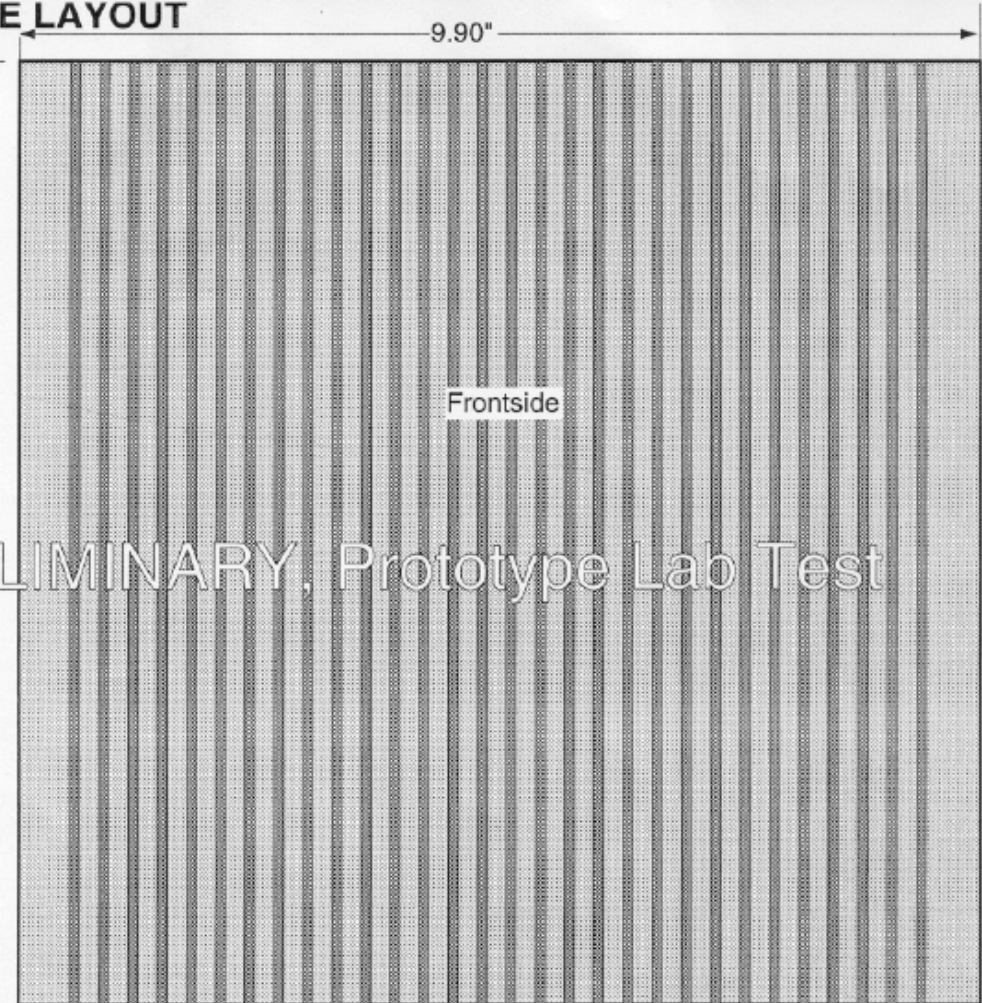
Motor

FANS

FANS

TEMP
 SENSORS

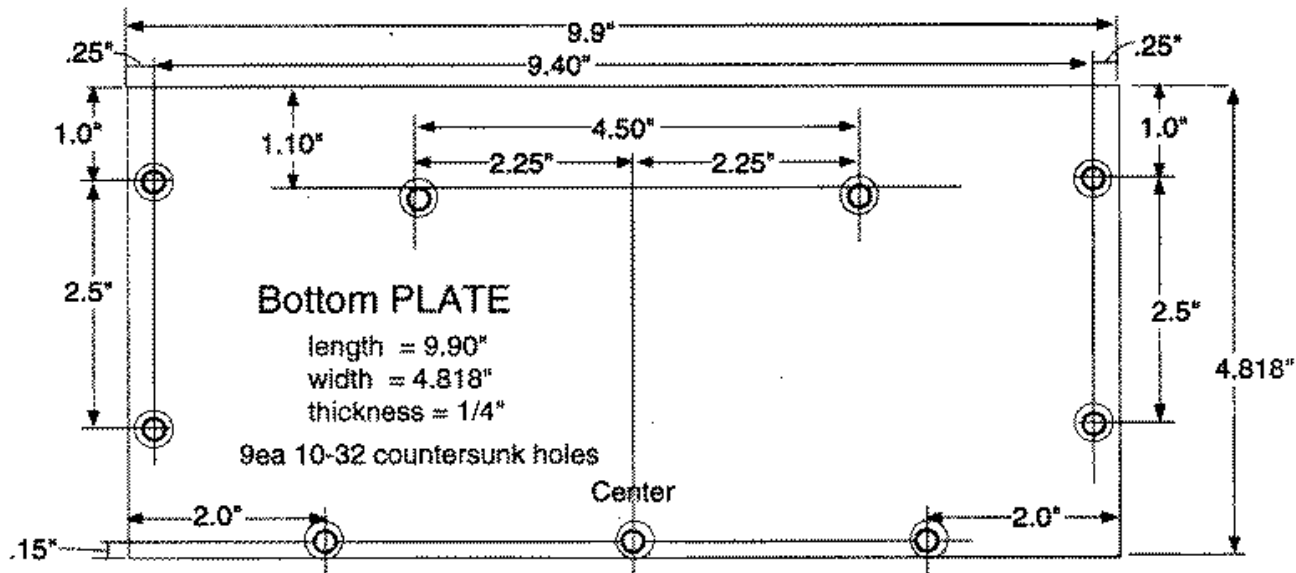
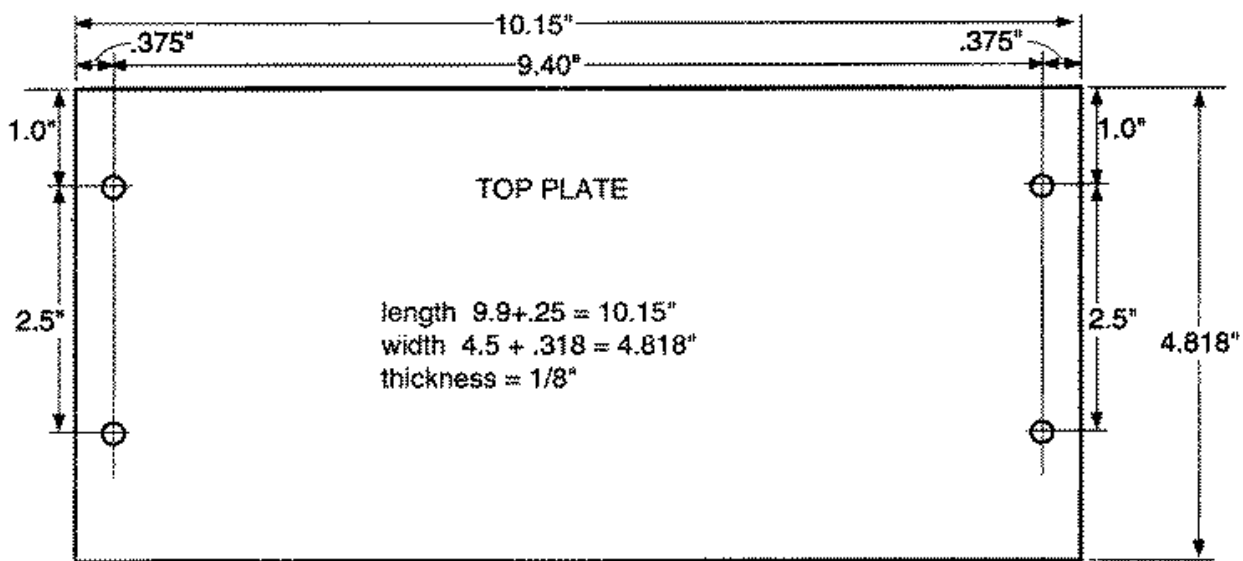
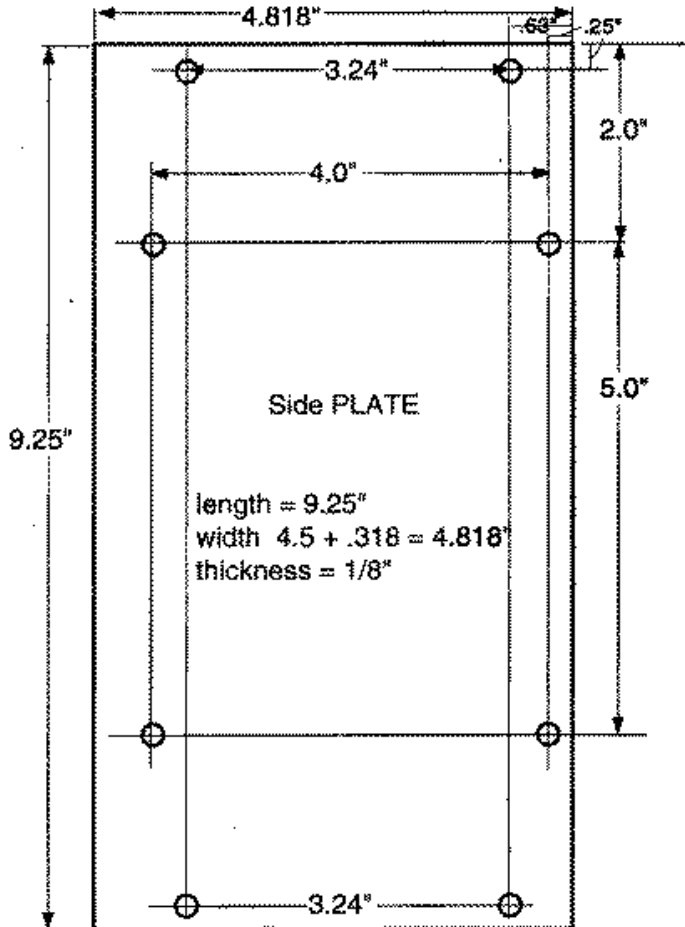




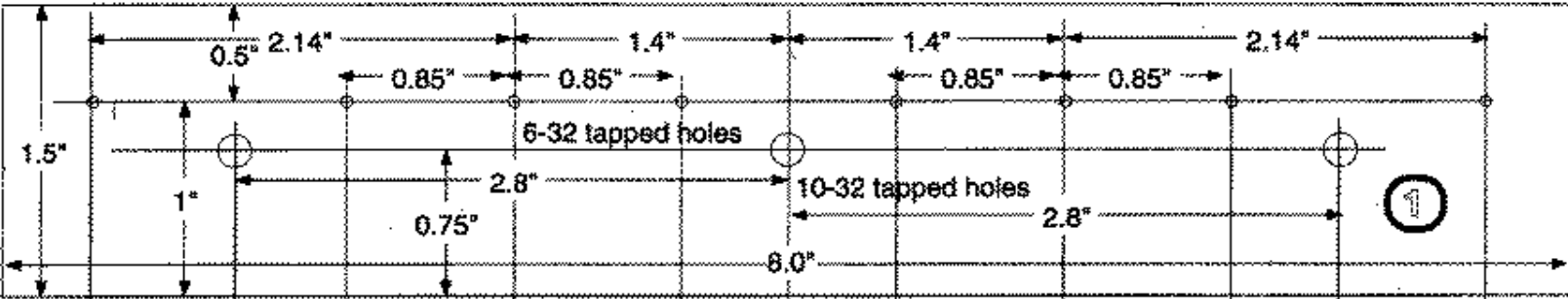
IGBT POWER MODULE LAYOUT

Top, Bottom, Sides

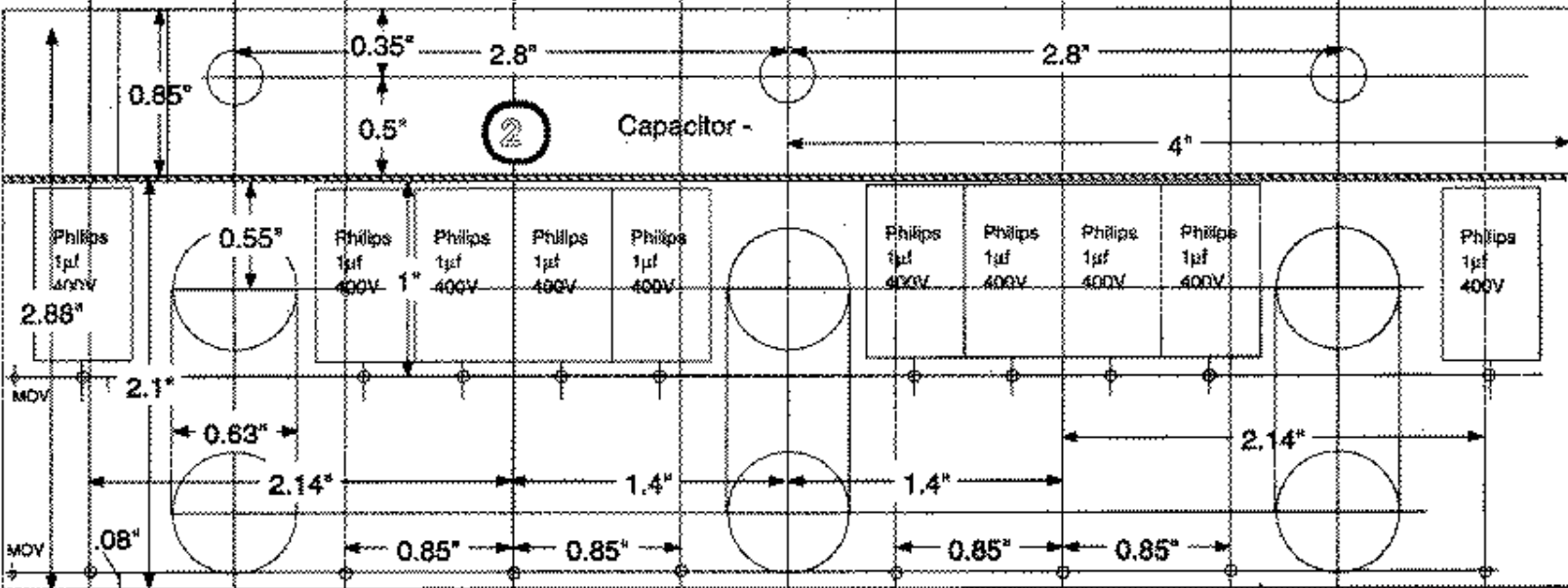
Page 6 of 10



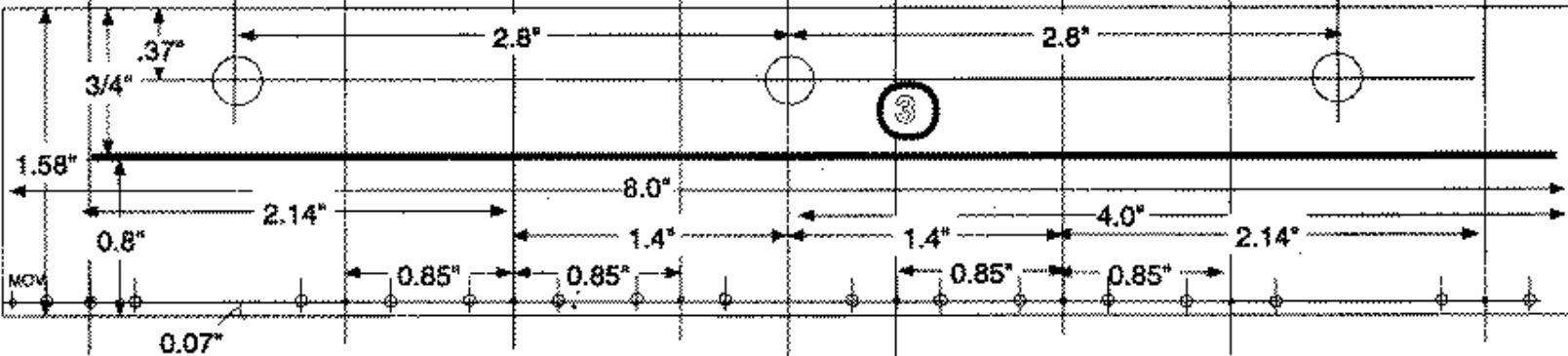
Rectifier Mounting Plate



Capacitors to Rectifiers, cathode plate



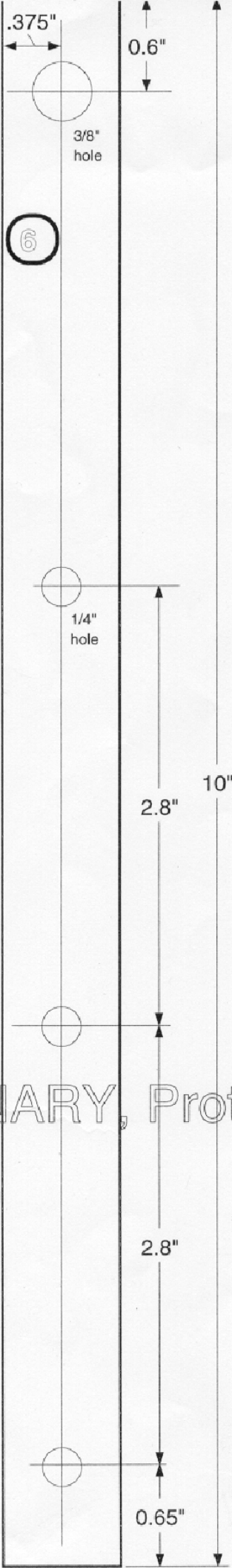
IGBT Drain to Rectifier (Anodes) Connecting Plate



IGBT POWER MODULE LAYOUT
Power Bars (3 each)
Page 9 of 10

375
250

250



PRELIMINARY, Prot

IGBT POWER MODULE LAYOUT

Metal Parts List

Page 10 of 10

Copper Plate, 1/32" Thick

Alum. Bar, 1/4" Thick

Alum. Plate, 1/4" Thick

Alum. Plate, 1/8" Thick

4ea. 6-32 x 1/4" brass screws

6ea. 1/4-28 x 7/8" bolts (Philips 3300µf Caps.)

8ea. 1/4-20 x .5" bolts (Rectifier Anodes)

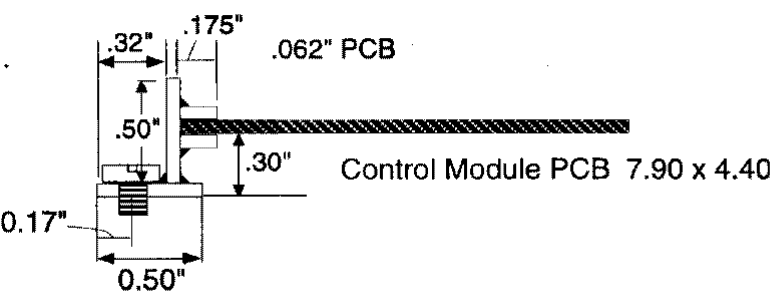
3ea. M6 x 17mm bolts (IGBT emitter)

3ea. M6 x 24mm bolts (IGBT Collector)

Construction Notes:

Align Up all similar patterns before drilling holes common to all pieces

Use Brass Hardware when available



Module Mounting Slider Brackets